Received: 9 December 2024 | Accepted: 22 March 2026

DOI: 10.1111/1365-2745.70344

Journal of Ecology

RESEARCH ARTICLE

A machine learning framework for mapping shifts in species' abundance from long-term monitoring data

Ilya Shabanov[1] | Andrew Lensen[2] | Jonathan Tonkin[3] | Julie R. Deslippe[1]

[1]School of Biological Sciences, Victoria University of Wellington, Wellington, New Zealand

[2]School of Engineering and Computer Science, Victoria University of Wellington, Wellington, New Zealand

[3]School of Biological Sciences, University of Canterbury, Christchurch, New Zealand

Correspondence
Ilya Shabanov
Email: ilya.shabanov@vuw.ac.nz

Funding information
New Zealand Tertiary Education Commission Centres of Research Excellence Fund, Grant/Award Number: E4050-3443

Handling Editor: David Armitage

Abstract

1. Climate change has driven extensive reorganisation of plant communities as species adjust their ranges in response to changing conditions. Existing studies focus on the role of temperature, documenting shifts in range margins, but neglect changes in abundance within the range. This results in unexplained patterns complicated by overlooked, interacting biotic and abiotic drivers, such as soil properties and herbivores, limiting our ability to predict forest response and vulnerability to climate change.
2. Here, we develop the Abundance Trend Indicator (ATI), a machine learning approach that learns the conditions under which changes in species' abundance have occurred and, thus, the extent and location of the mismatch of a species' current range to its total realised habitat. The resulting abundance shift maps identify abundance shift directions, vulnerable species and their drivers. We validate the algorithm on New Zealand's forest inventory data (2821 sites, 77 woody species, collectively accounting for 75% of forest canopy nationally) and 37 predictor variables, which include climatic, topographic, edaphic and biological factors.
3. ATI confirms globally observed trends of upward and poleward abundance shifts, but reveals drivers such as soil pH, grazing and climate stability for species shifting in opposite directions. Moreover, our findings suggest that vulnerability is primarily explained by a plant's ability to tolerate or avoid stress resulting from climatic fluctuations and limited migration capacity.
4. *Synthesis*. Using existing forest inventory data, ATI models within-range abundance shifts, rather than changes in range margins, resulting in earlier detection of environmental drivers and geographical directions of plant migration. This enables the early identification of vulnerable species.

KEYWORDS
biogeography, climate change, climate vulnerability, forest inventory data, machine learning, New Zealand forest, range shifts, species distribution models, tree population dynamics

1 | INTRODUCTION

Human activities drive climate change, biodiversity redistribution and species introductions that are reshaping Earth's ecosystems at an unprecedented rate and creating novel climates (Williams et al., 2007) and communities (Gougherty et al., 2024). Species react to these environmental changes by expanding or contracting their geographical range, tracking more favourable conditions or persisting in place due to phenotypic plasticity, genetic adaptation (Diamond, 2018) or phenological shifts (Jakoby et al., 2019). Failure to adapt or migrate leads to various degrees of vulnerability or extinction (Lenoir & Svenning, 2015). Identifying the behaviour of species in relation to their biotic and abiotic environment, therefore, is key to conserving biodiversity.

The most well-documented trend of species range shifts (~50%–80%) in response to recent climate change is a poleward and upward movement towards cooler temperatures (Lawlor et al., 2024; Rubenstein et al., 2023). Fewer than 20% of studies consider range-shift drivers beyond temperature (Taheri et al., 2021). Temperature, however, might not be a direct driver of range shifts. For example, the water balance of individual trees is influenced by factors such as topography, soil and interspecific interactions (Stephenson, 1998), making range shifts inherently local (Rapacciuolo et al., 2014). Consequently, many species may be responding not to temperature itself, but to other changing environmental factors, such as precipitation (Crimmins et al., 2011; Fei et al., 2017), biotic interactions (Lenoir et al., 2010; Louthan et al., 2015) or land-use change (Guo et al., 2018). Accurate range shift analyses, therefore, need to consider multiple drivers as well as their interactions (Lawlor et al., 2024).

In long-lived plant species, range shifts often lag behind within-range abundance shifts (Breshears et al., 2008), sometimes by centuries (Beckage et al., 2008), thereby masking the responses to climate change. Previous studies, however, have mainly documented range shifts at species' margins (Lenoir & Svenning, 2015) as they only require presence–absence data. This neglects that a plant species' demographic performance varies across its geographical range, in response to local abiotic gradients (Doak & Morris, 2010; Lynn et al., 2021; Villellas et al., 2015). Abundance shift observations across the species' entire range should therefore be preferred to range shift observations to assess climate change responses and identify vulnerable species.

Plant abundance and occurrence data are available from National Forest Inventories (NFIs), which monitor forest composition over time (Tomppo et al., 2009). However, these inventories often lack uniform methods for collecting, storing and processing this data, especially for older observations (Chirici et al., 2012). New analytical approaches can unify conflicting protocols and handle missing data. For instance, seedlings and adults are usually surveyed using different methods (Wiser et al., 2001), but comparing their distributions can be used for range-shift assessments (Lenoir et al., 2009; Woodall et al., 2009). In another instance, to account for heterogeneous survey methodologies, multiple locations were combined into an artificial plot and abundances compared to reveal shifts and drivers of change (Fei et al., 2017). Analytical methods, therefore, will leverage larger datasets and yield more widely applicable insights if they are able to operate on protocol-independent representations of NFI data rather than relying on inventory-specific survey designs.

The most common methods used to assess range shifts are species distribution models (SDMs, Guisan & Thuiller, 2005), which model the abiotic conditions of a species' presence and extrapolate it into the future (Foden et al., 2019). Since SDMs typically output habitat suitability, they fail to reliably predict abundances needed for effective conservation (Johnston et al., 2015), with only 42% of studies finding consistent positive correlations with independent abundance estimates (Lee-Yaw et al., 2022). Abundance can also be predicted by demographic rates (Ehrlén & Morris, 2015) through process-based models (Connolly et al., 2017), but estimating them requires data of high spatiotemporal resolution (Dormann et al., 2012) and, for long-lived trees, in particular, at different life stages (i.e. stage-dependent population models Caswell, 2006). Despite growing data availability (e.g. COMPADRE database, Salguero-Gómez et al., 2015) data on vital rates remain scarce. For instance, COMPADRE contains only three native vascular plant species from New Zealand. More data and better methods are therefore needed to overcome these challenges and better predict the impact of climate change on species range and abundance shifts (Lenoir & Svenning, 2015).

Here, we present a conceptually distinct machine learning approach, the 'Abundance Trend Indicator (ATI)', which estimates the degree to which a specific climate is conducive to an increase in species abundance. The resulting ATI maps allow for estimation of geographical abundance gradients and numerous environmental drivers of these abundance changes. Moreover, vulnerability can be assessed if the abundance trend of a species is predominantly negative. We validate and exemplify the approach using New Zealand's forest inventory dataset comprised of 2821 sites surveyed from 1969 to 2019 with individual counts of 77 woody species and 37 spatio-temporal, abiotic and biotic variables. We aimed to quantify the contribution of drivers other than temperature to abundance shifts, distinguish individual species responses from mean trends and assess species vulnerability arising from species-specific environmental limits and stressors. Detailed species-level results and ATI maps are available on an interactive website: https://ati-nz-predictions-7e6f3d514735.herokuapp.com/.

2 | MATERIALS AND METHODS

The Abundance Trend Indicator (ATI) is a machine learning model that uses environmental (i.e. biotic and abiotic) predictor variables x_i to predict how conducive a location i is to a species abundance increase (Figure 1). It is trained on resurveyed plots where the binary target labels $y_i \in \{0, 1\}$ corresponded to an increase or decrease of individual adult tree counts (steps 1 and 2 in Figure 1). Formulating y as a binary variable allows us to clean the training data using a well-established framework (Brodley & Friedl, 1999) (step 3) and to achieve higher accuracy in predicting y from x (step 4). The

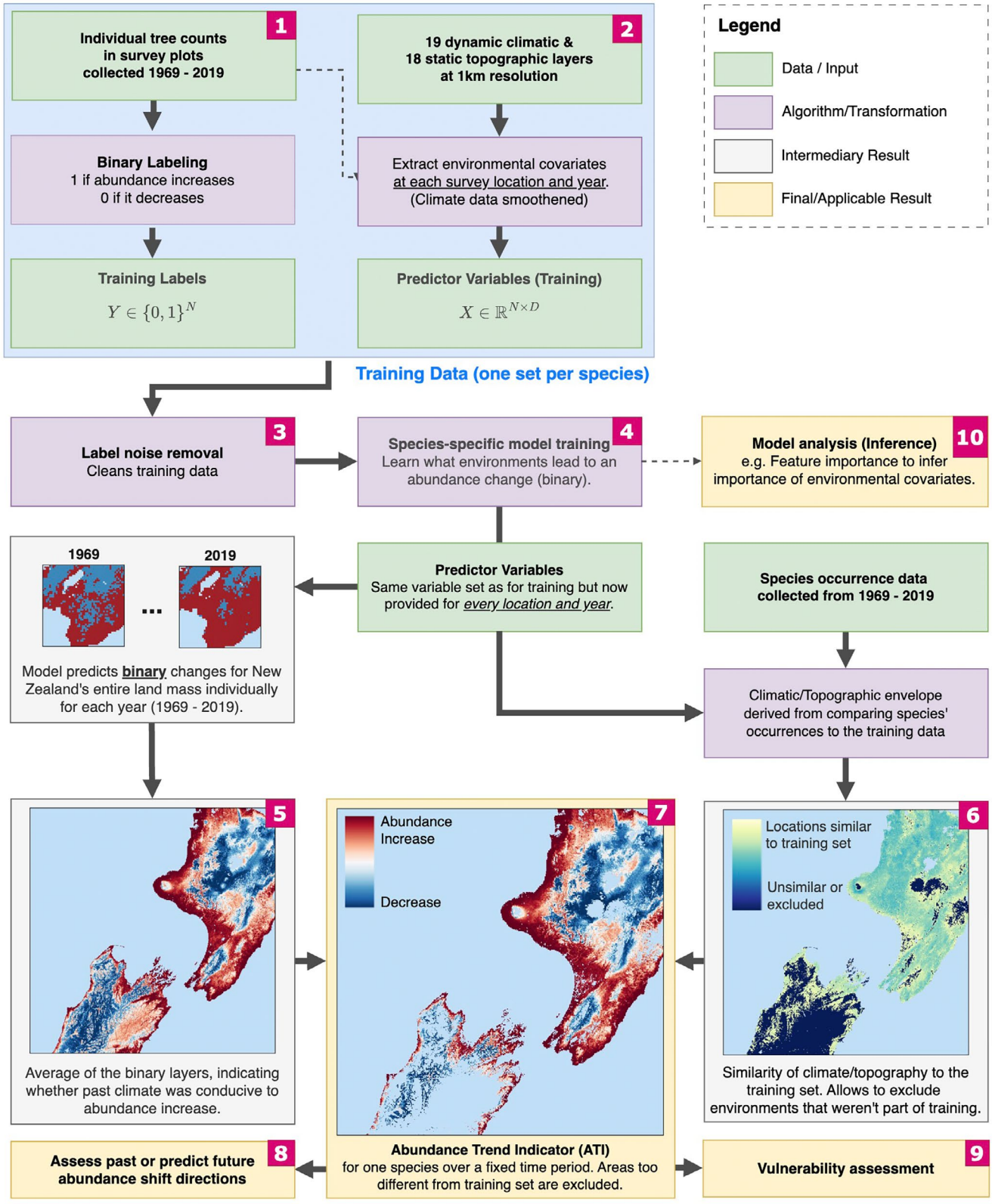

FIGURE 1 Overview of the Abundance Trend Indicator (ATI) algorithm. The final ATI map (step 7) is the combination of the predictions of a (binary) classification model trained on tree count data and environmental variables (left path, steps 1–5) masked by areas similar in climate and topography to the training data (right path, step 6). ATI maps reveal environmental and geographical gradients of abundance shifts and species vulnerability (steps 8–9). Additionally, models can be analysed directly (step 10) to infer the importance of environmental covariates. A dashed line between steps 4 and 10 indicates that the models from step 4 are used for inference in step 10.

model, then, made binary yearly predictions over the species' entire range $\text{ati}_{yr}: \mathbb{R}^{N \times D} \rightarrow \{0,1\}^{N}$, which were averaged over the years 1969–2019 (step 5). This step transformed binary into continuous predictions, indicating how conducive the environment in each grid cell was to abundance increases over the 50-year period. To avoid extrapolation, we limited predictions to the range of environmental conditions where the species has been previously observed (step 6). The final ATI map (step 7) thus consisted of the ATI predictions (step 5) masked with the similarity mask (step 6) and was used to reveal directions of increasing abundance (abundance gradients, along geographical or environmental variables) and assess how favourable a species' realised niche is to increased abundance (i.e. vulnerability, steps 8 and 9).

2.1 | Occurrence dataset and training labels (step 1)

New Zealand, as a study area, is well-suited for studying climate-driven abundance shifts because its forests span a wide range of latitudinal, elevational and temperature gradients (see Figure 3) with intact forests largely managed for conservation (Ewers et al., 2006; Heino et al., 2015). The Southern Alps, spanning almost the entire length of the South Island, encompass alpine flora, cool-temperate forests and lowland shrublands, whereas in the north, the vegetation transitions from montane to subtropical. Long geographical isolation results in a very high level of endemism (82% of plant species, Murray & de Lange, 2011), many with limited dispersal capacity and distinct ecological strategies, which makes within-range demographic responses particularly informative (Pagel et al., 2020). In addition, introduced herbivores (e.g. red deer Forsyth et al., 2010) impose spatially heterogeneous top-down pressure on forest vegetation, providing an opportunity to assess how biotic regulation interacts with climatic gradients to shape climate change responses (Jia et al., 2018).

A training label is a binary number that refers to an outcome a model aims to predict, given a set of predictor variables (e.g. an increase or decrease in abundance under certain environmental conditions). To obtain training labels for our model, we used a subset of 2821 plots in New Zealand's nationwide forest inventory data (NVS, Wiser et al., 2001) containing 311 woody species with at least two surveys in the years 1969–2019, not more than 30 years and not less than 2 years apart (9388 observations total). Importantly, this dataset contains a series of permanent plots covering all forested areas at regular spatial intervals, minimising spatial bias (visible as a grid pattern in Figure S6). Moreover, the protocol ensures a consistent measurement of vegetation. Each plot measured 20 × 20 m. If a plot was measured more than twice, each consecutive pair was treated independently. Each survey consisted of counts of mature individuals of shrubs, trees, tree ferns and vines, and their diameter at breast height (DBH). Individuals under 120 cm in height were not counted. Plots closer together than the resolution of our topographic data (100 m) were treated as one combined plot.

We used two methods to extract training labels, resulting in two datasets:

1. Abundance Only: Based on whether the number of individuals increased or decreased, a 1 or 0 was assigned. Instances with an equal number of individuals were discarded.
2. Abundance and DBH: Expands the Abundance Only datasets by adding plots with an unchanged number of individuals, where a 1 was assigned if the sum of DBH of all individuals increased. In 74.9% of cases, equal individuals resulted in a DBH increase (i.e. individuals aged and grew). In 25.1% younger individuals replaced older individuals, and total DBH decreased.

The datasets yielded 65 species covering 69.37% and 86 species covering 75.59% of forest canopy cover, respectively (Figure S1). The Abundance Only dataset records a '1' only when individual counts rise due to recruitment, survival or reduced mortality. The Abundance and DBH dataset broadens the criteria for a positive abundance trend by including an increase in biomass (i.e. an increase in total DBH, but not individuals).

We used another subset of NVS plots measured using the RECCE methodology (Hurst, 2022; 18,664 observations in 15,095 plots) to estimate species cover, as they contained categorical cover estimates for every height tier category (1 through 6, for individuals >25 m down to <60 cm) and can be collapsed into a single cover estimate (Fischer, 2015). The sum of these estimates was normalised to 1, yielding relative canopy cover values for each species. Given that abundance changes are approximately Gaussian distributed (Figure S9) and following (Pearson et al., 2007; Wisz et al., 2008), we excluded species with fewer than 100 total or fewer than 20 observations in either class to avoid a strong class imbalance and an over-dependency of scores on the random choice of training and test data.

2.2 | Predictor variables and training data (step 2)

We derived predictor variables from geospatial data. Variables that change over time (e.g. climate) need to be provided for each year, as otherwise ATI predictions would be identical every year and result in a binary output (see grey box between steps 4 and 5 in Figure 1). We constructed 19 BioClim variables (O'Donnel & Ignizio, 2012) obtained from monthly rainfall, minimum and maximum temperatures at 1 km resolution from the HOTRUNZ dataset (Etherington et al., 2022). We then decomposed the time-dependent BioClim variables $v(t)$ into a linear trend and a stochastic component: $v(t) = m_v \cdot t + \eta$ retaining only the former for training. This reduces the effect of annual climate fluctuations on species abundances in favour of slow decadal climate changes. Short-term fluctuations, however, are captured in dedicated BioClim variables, such as temperature seasonality. Additionally, we extracted 15 static topographic and edaphic variables (e.g. elevation) from the NZEnvDS dataset (McCarthy et al., 2021). Since New Zealand's vegetation

is subject to strong impacts from grazing by introduced mammals (Wyse et al., 2018; Zotov, 1938), we included layers for rat, possum and red deer distributions (Department of Conservation, 2015a, 2015b, 2015c).

We reduced the 'Full' 37-variable dataset to an 'Explain' 14-variable dataset using hierarchical clustering (see Section S1.2, Figure S2 and Table S1) to improve the interpretation of climatic drivers by removing highly correlated variables. Limiting collinearity additionally improves the fidelity of feature importance scores (Section 2.10; Molnar, 2022). PCA was considered but discarded due to poorer model performance and interpretability (Figure S3). For applications where variable interpretation is secondary to model performance (e.g. spatial forecasting of locations of high canopy turnover), the 'Full' dataset can be used, as it yields a slightly better model fit (Figure S12). However, since our focus was on obtaining ecologically interpretable results, we used the 'Explain' dataset for this study. The interactive website contains results for both datasets (https://ati-nz-predictions-7e6f3d514735.herokuapp.com/).

Because the model is trained to predict changes in abundance, it may be susceptible to regression to the mean (RTM), where extreme initial values can create spurious correlations with environmental predictors (see Section S1.7 for details). A common mitigation strategy is to include the initial abundance as a covariate (Mazalla & Diekmann, 2022). However, in our case, an initial abundance of zero would always produce a binary 'increase' label, thus revealing the labels in the training data and artificially inflating model performance. We therefore included mean abundance instead. Since abundance is only known for the training data, this adjustment can only be applied for inference (only Section 2.8 and Figure 5), not for prediction. Overall, ATI's binarisation reduced RTM effects to a negligible level ($R^2 \approx 0.01$; Figure S8 and Section S1.7).

2.3 | Data cleaning (step 3)

Our dataset contained data entry and collection errors (see Section S2), leading to erroneous target labels (i.e. labelling noise). Such issues are common in multi-decadal national forest inventories, where observer changes, taxonomic revisions and disturbances introduce inconsistencies (Thompson et al., 2007). In our data, at least 2.7% of plots had unnaturally high species turnover, and 3.68% of congeneric species were misidentified. Labelling noise can also arise from the stochasticity of rare or hard-to-detect species, resulting in reported error rates of 5.9% to 21% (Scott & Hallam, 2003; Verheyen et al., 2018). To reduce labelling noise, we modified an established editing procedure (Frénay & Verleysen, 2014) to allow the exclusion of a flexible number of potentially erroneous observations. We found an effective cut-off rate of 10% and 15% for the Abundance Only and Abundance and DBH datasets, respectively (Figure S12C). Beyond these thresholds, the cleaning process rendered some species data-deficient, thereby reducing the dataset.

Our algorithm assigned each data point (i.e. plot pair) a continuous noise score $\epsilon_i \in [0, 1]$ based on its environmental predictors x_i and binary label y_i, relative to the K most similar neighbouring plots and their labels. Similarity was defined as the sum of differences of all environmental variables. High noise scores indicated plots whose labels contradicted those of environmentally similar neighbours (Figure S4). Ranking observations by noise scores allowed for the flexible removal of the noisiest fraction of the dataset. Section S1.3 provides a detailed description of the data cleaning steps.

2.4 | Model training (step 4)

We used a random forest (RF) classifier implemented in the SciKit Python package (Pedregosa et al., 2011), due to its excellent predictive performance (Breiman, 2001). Random forests classify data by aggregating predictions from many decision trees built during training. Three alternative models: logistic regression, support vector machines and artificial neural networks showed poorer performance (Figure S12) and were not pursued further (see Section S1.4). We identified optimal hyperparameters using an exhaustive grid search across all possible parameter combinations (Table S2). Model training employed fourfold cross-validation, and predictive performance was evaluated using the mean Area Under the Receiver Operating Characteristic Curve (ROC AUC) (Fawcett, 2006). In ecological applications, ROC AUC values below 0.7 are generally considered poor (Araújo et al., 2005). We therefore rejected classifiers scoring below this threshold. Final model performance was calculated as the average ROC AUC score of the four test folds (see Table S5).

2.5 | Unmasked ATI maps (step 5)

The trained models make discrete predictions for each grid cell i and year $\text{ati}_{\text{yr}}: \mathbb{R}^{N \times D} \rightarrow \{0, 1\}^N$. Taking the average over all years $Y = \{\text{yr} |\ 1969 \leq t \leq 2019\}$ yields a single continuous number between 0 and 1 $\text{ATI} = \frac{1}{|Y|} \sum_{\text{yr}} \text{ati}_{\text{yr}}$ for each grid cell i. This eliminates species-specific differences in the number or spacing of training data points. The predictions can be mapped. Locations with ATI <0.5 indicate that environmental conditions averaged over the years Y led to a decrease in abundance, whereas locations with ATI >0.5 indicate that conditions led to an increase in abundance. Importantly, the unmasked map contains areas far outside the training range (i.e. a species' realised niche), possibly leading to erroneous model behaviour (Bartley et al., 2019). We therefore discarded predictions outside the species range (see next section).

2.6 | Similarity maps (step 6)

Following (Owens et al., 2013), we identified and excluded grid cells whose environmental conditions fell outside those represented in the observed species records, thereby avoiding extrapolation into novel environmental space. The resulting binary similarity masks delineated each species' realised range, allowing a small, flexible

margin around the observed conditions (Figure S6). First, to assess how similar environmental conditions at a location x_i were to those at the observed locations, we calculated the average distance in terms of environmental similarity to the $K = 3$ nearest observed locations $NN(x_i)$ for each year individually and then averaged over all years, yielding $D_i = \frac{1}{|Y| \cdot K} \sum_{y \in Y} \sum_{x \in NN(x_i)} \|x - x_i\|_1$. The result is a distance map (Figure S6A) that assigns an environmental distance value to each grid cell i. Next, we defined a threshold S per species and excluded points where $D_i > S$. This yielded the binary similarity mask (Figure S6C). We defined $S = \gamma S'$ with $\gamma = 1.2$ (Figure S6C yellow area) where S' is the threshold containing 95% of a species occurrences (Figure S6B) and corresponds to the range of the species without strong outliers (Figure S6C orange area). However, since we are interested in predicting range shifts beyond the observed range, we set $\gamma > 1$ to include the periphery of the species range (Figure S6C, yellow area added due to $\gamma > 1$).

2.7 | Final ATI map (step 7)

The final ATI map (Figure 1, Step 7) comprises modelled predictions with environmentally dissimilar areas removed using the similarity mask (see previous two sections). This map indicates how frequently climatic conditions over the past 50 years have facilitated increases in abundance within and immediately surrounding a species' realised niche. The spatial mean of the ATI map provides an overall indicator of the species' climatic vulnerability, while its spatial gradients indicate the direction of abundance shifts. Interpretation depends on the training dataset used (see Section 2.1). We use the Abundance Only dataset to infer abundance gradients, as it provides a stronger signal of demographic expansion. For climate vulnerability assessments, we used the larger Abundance and DBH dataset. The difference between the datasets is that ATI >0.5 in the former suggests increasing population size, whereas in the latter, it reflects either population expansion or biomass growth (i.e. increased DBH without an increase in the number of individuals).

2.8 | Abundance gradients (step 8)

Abundance shifts are defined as transitions from areas of predicted decline to areas of predicted increase. These directions can be analysed along geographic gradients to determine where species are moving (e.g. to lower latitudes) or along environmental gradients to identify the climatic or biotic drivers of the abundance shift (e.g. towards lower temperatures, niche shifts). To quantify these directions, we first segment the grid cells in the ATI map into two subsets: $\text{ATI}^+ = \{i \mid \text{ATI}_i > 0.5\}$ and $\text{ATI}^- = \{i \mid \text{ATI}_i \leq 0.5\}$ which correspond to spatially explicit areas of projected demographic gain or loss, respectively.

Next, for a variable of interest v, we calculate its average value within each subset, weighed by the predicted ATI values: $\mu(v)^+ = \frac{1}{|\text{ATI}^+|} \sum_{i \in \text{ATI}^+} \text{ati}(i) \cdot v(i)$ and analogously for $\mu^-(v)$. These weighted means reflect the average conditions associated with predicted increases or decreases in abundance, respectively. Therefore, we can interpret the difference $\Delta v = \mu^+(v) - \mu^-(v)$ as an abundance gradient along the variable v. For example, if v is elevation and $\Delta\mu(v) > 0$, the abundance gradient points towards a higher elevation, indicating an uphill migration. If v is precipitation, the species expands into wetter climates (e.g. to escape an arid climate). Importantly, abundance gradients are not range shifts, which are defined geographically. Rather, they describe the environmental or spatial direction within and around the realised niche towards which the abundance is predicted to increase. To synthesise patterns across variables, we used principal component analysis.

2.9 | Climate vulnerability assessment (step 9)

To assess species' vulnerability to climate-related extinction (hereafter: 'vulnerability'), we computed the mean ATI across all predicted grid cells using the Abundance and DBH dataset. A median value <0.5 indicates that predicted decreases outweigh increases within the species' realised range. To estimate overall forest condition, we computed a canopy-weighted average ATI across species, using relative cover as weights. This provides an integrated indicator of forest demographic health. ATI value distributions will have heavy tails at the lower end, as the similarity mask allows for a slight extrapolation (factor $\gamma = 1.2$ in Section 2.6) outside of a species' realised niche (Figure S6), which would naturally have very low ATI values. When assessing vulnerability, a slightly smaller quantile (e.g. 25%–75% in Figure 2), therefore, better approximates the ATI values within the species' currently occupied range. To interpret the drivers of vulnerability, we combined feature-importance scores (Section 2.10), which quantify the relative contribution of each predictor, with abundance gradient analyses (Section 2.8), which indicate the direction of demographic change along environmental axes.

2.10 | Feature importance (step 10)

Random forest models produce a positive feature importance value for each variable during training. These values sum to one and indicate the relative contribution of each variable to make correct predictions (Breiman, 2001). We used SciKit's Python package to extract these values for our models. For the feature importance analysis, we added the species abundance as an additional variable, as this eliminates the regression to the mean (RTM) effect, which confounds inference (Mazalla & Diekmann, 2022) (See Section S1.7 for details).

As environmental conditions relevant to a species' growth are expected to correlate well with the abundance trend, we computed correlations $r_s(v) \in [-1, 1]$ between ATI values and predictor variables v for every species s as an alternative importance metric. To highlight only the correlation's strength (and not the direction),

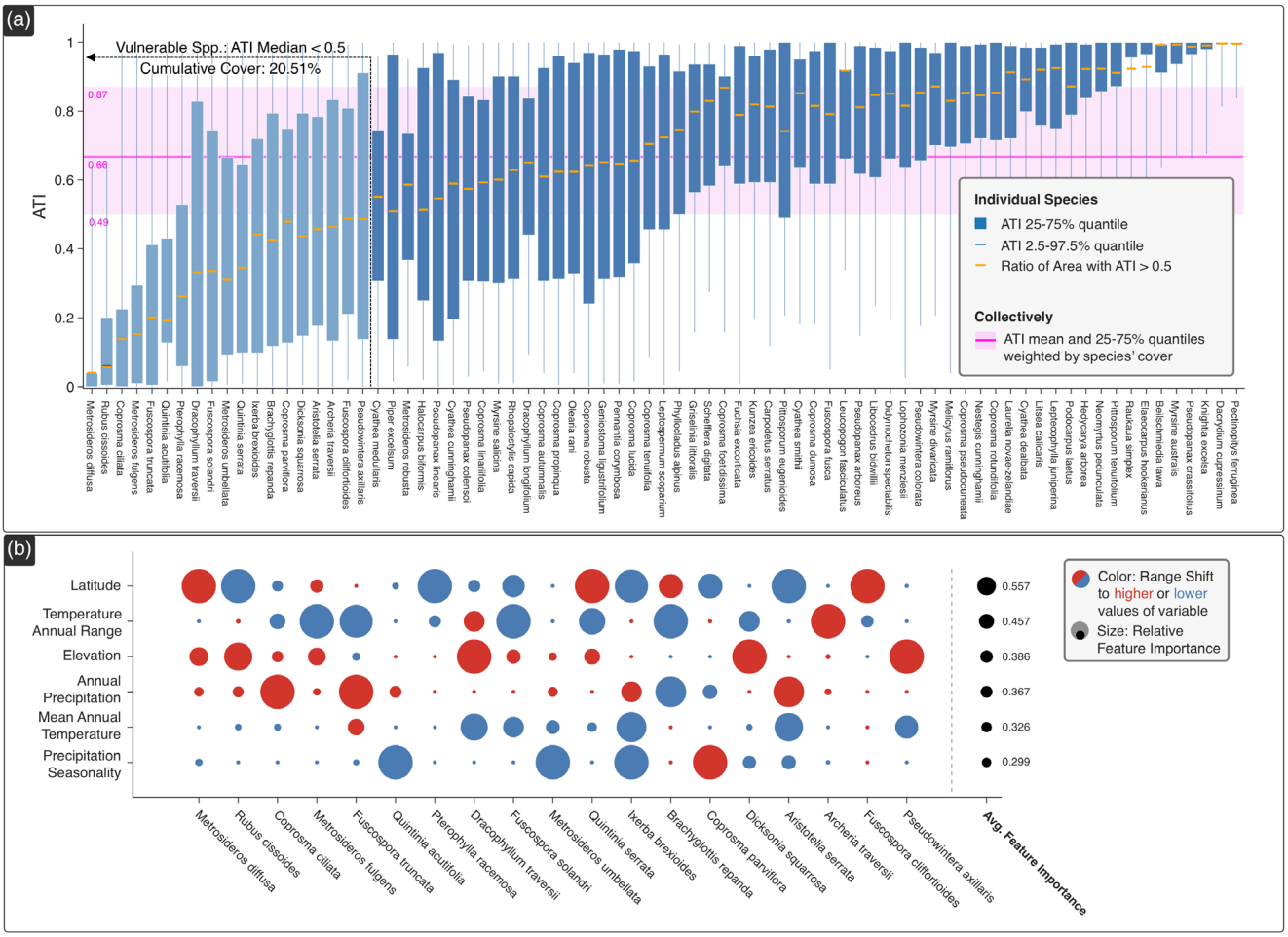

FIGURE 2 Vulnerability assessment through analysis of ATI distributions. (a): Bars indicate 25%–75% percentiles of ATI values across individual species' realised niches. Yellow lines indicate the ratio of grid cells with ATI >0.5 to total cells. The magenta line is the cover weighted mean for all species. Nineteen vulnerable species (light blue bars) have an ATI median below 0.5. (b): Feature importances and abundance gradients for the 19 vulnerable species. The size of markers indicates the importance of the feature for the species' model. Colours indicate abundance increases (red)/decreases (blue) towards larger values of this variable. The right column gives the average importance of each variable for all species.

we use the absolute value of the correlation $|r_s|$. To assess the importance of a variable in general, we average it across all species $|\tilde{r}(v)| = \frac{1}{N}\sum_s |r_s(v)|$.

2.11 | Synthetic species

To illustrate our method's applicability and correctness, we generated three synthetic species shifting their abundance exclusively up a precipitation, elevation or latitude gradient. We compared AUC scores of the synthetic predictions to those of natural species, presumably driven by multiple environmental drivers and their interactions.

Two Gaussian distributions (for the year 1990 and 2019) described the synthetic species' abundance distribution along each variable. The mean of these distributions was artificially offset to mirror globally observed speeds of range shift for latitude and elevation of 11.8 km/decade and 9 m/decade (Rubenstein et al., 2023). We used real-world climate data for this experiment. A detailed description is provided in Section S3.4.

3 | RESULTS

3.1 | Assessing species' climate vulnerability

We identified 19 vulnerable species for which, on average across their ranges, observed environmental change has led to declines in their abundance over the study period (i.e. median ATI <0.5, Figure 2a). These species had a collective canopy cover of 20.51%. Across all 86 species, however, the ATI median was 0.66, indicating that collectively, recent environmental change contributes to increases in New Zealand's species richness locally. The climatically vulnerable species were predominantly predicted to shift their abundance towards higher elevation and precipitation and towards

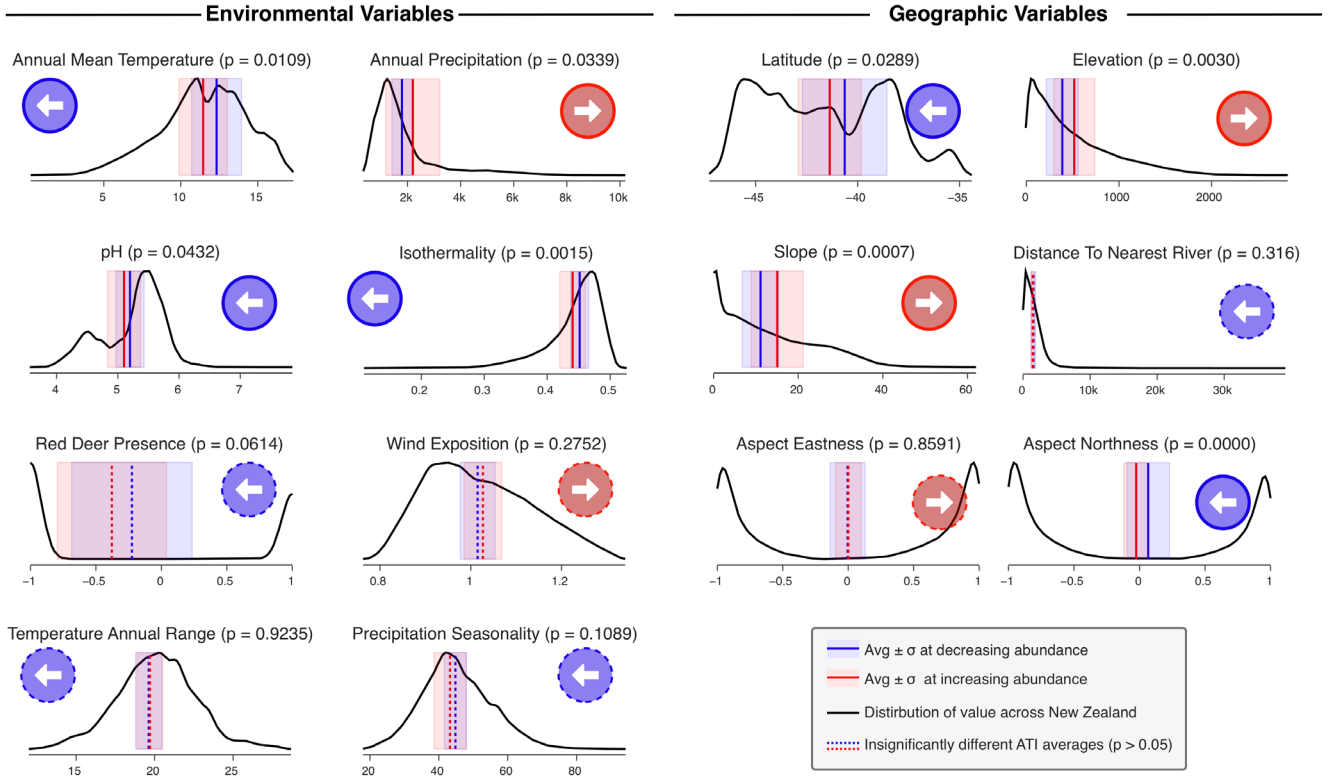

FIGURE 3 Each subplot corresponds to abundance gradients along one environmental variable (e.g. Elevation, top right) and shows the average conditions correlated with increasing (red vertical line) and decreasing (blue vertical line) abundance trend prediction across all species. The shades represent ±1 the standard deviation among all 62 species. An arrow depicts the direction of the gradient along this variable (e.g. points rightwards, towards higher elevation). Dashed arrow outlines signify statistically non-significant changes. The black line indicates each variable's nationwide (New Zealand) distribution to provide context for the frequency of the habitat.

lower temperature and precipitation fluctuations (Figure 2b). The most important directions of abundance changes occurred along latitude and temperature ranges. For four species, however, abundance shifts occurred along a precipitation seasonality gradient, an otherwise less important variable.

3.2 | Abundance shifts polewards and upwards towards steeper, wetter, cooler areas with lower isothermality

We identified abundance gradients for 62 species in the Abundance Only dataset (Figure 3). In addition to abundance gradients along elevation, temperature and precipitation, we found statistically significant abundance shifts (see Table S6 for test statistics) in the direction of areas with lower isothermality, more acidic soils and steeper slopes. Since the annual temperature range (a component of isothermality) showed no significant shifts, isothermality gradients might be explained by lower diurnal ranges. Precipitation seasonality, wind exposure and the distance to the nearest river were not associated with significant shifts in abundance. While species preferred the absence of red deer, the difference was non-significant across all species. Aspect showed no significant gradients along eastness but a small, significant shift along northness, corresponding to a rotation of ~5° closer to cooler, south-facing slopes.

3.3 | Species respond individually to climate change and are far from the mean

For the six variables with the strongest abundance gradients, we additionally assessed the distribution of individual responses and compared them to the mean response (Figure 4a–c). Across all six variables except precipitation seasonality, approximately two thirds of species shifted in the average direction. For example, 63.8% of species shifted their abundance towards the average direction of wetter habitats, and 65.5% towards cooler habitats (i.e. towards the lower left of Figure 4a). The remaining ~35% shifted into drier and warmer habitats. Likewise, 69.9% and 67.9% of species increased abundance polewards or towards higher elevations, respectively (i.e. towards the bottom and right of Figure 4b). The mean and standard deviation of responses across all species (red cross and ellipse, Figure 4a–c) only poorly captured the accurate distribution of

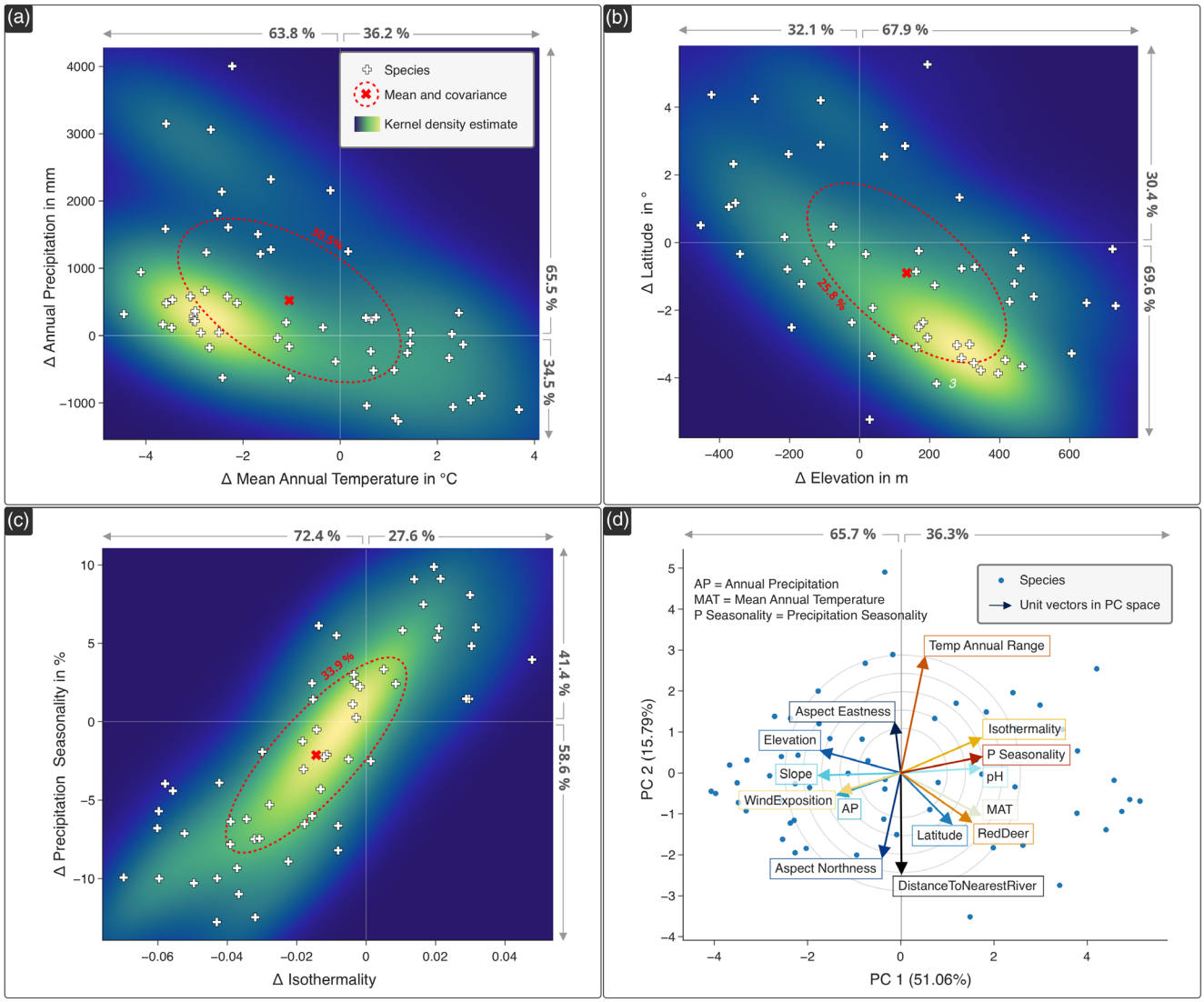

FIGURE 4 Abundance shift directions for single species. (a–c): Points are single species, and values on the axes give the difference in average conditions between areas of ATI >0.5 (increasing abundance) and ATI ≤0.5 (decreasing abundance). For instance, if Δ Elevation = 100 m, areas of decreasing and increasing ATI are on average separated by 100 m in elevation. Background heatmap is a kernel density estimate across all species and is brighter in areas with more species. The mean and one standard deviation ellipse are shown in red. (d) PCA biplot of abundance gradients along all 14 environmental variables, concentric circles for length comparison of unit vectors.

individual shifts (background heatmap), indicating species-specific rather than collective responses.

A principal component analysis of all abundance gradients resulted in a dominant axis (PC1, explaining 51.06% of variation, Figure 4d). Negative values on PC1 described abundance gradients aimed polewards, towards higher elevations and cooler climates, but also to harsher conditions (i.e. steeper, wind-exposed slopes and acidic soils). Positive values on PC1 reflected abundance gradients towards locations of stronger annual precipitation seasonality in precipitation and isothermality, and high grazing pressure and temperatures. Greater isothermality along PC1 is likely the result of increased diurnal ranges, as the annual temperature range is orthogonal to PC1. PC2 explained only a negligible 15.79% and was dominated by the temperature annual range and the distance to the nearest river (Figure 5b).

3.4 | Elevation and temperature insufficiently explain abundance shifts

To understand which variables drive abundance increases, we assessed ATI correlations and feature importance scores (Figure 5). While changes in species' abundance correlated most strongly with annual mean temperature ($|\tilde{r}| = 0.40$), elevation ($|\tilde{r}| = 0.34$) and latitude ($|\tilde{r}| = 0.32$), almost all remaining climate and soil variables were comparably highly correlated (0.31 to 0.1). In contrast, the three synthetic species (Section 2.11 and S3.4) correlated with their main abundance driver elevation ($r = 0.75$), annual precipitation ($r = 0.63$) and latitude ($r = 0.81$) substantially better than any real-world species (green diamonds, Figure 5a). Feature importance (Figure 5b), attributed comparably large importance to latitude, temperature, precipitation and their fluctuations. However, individual species' responses are

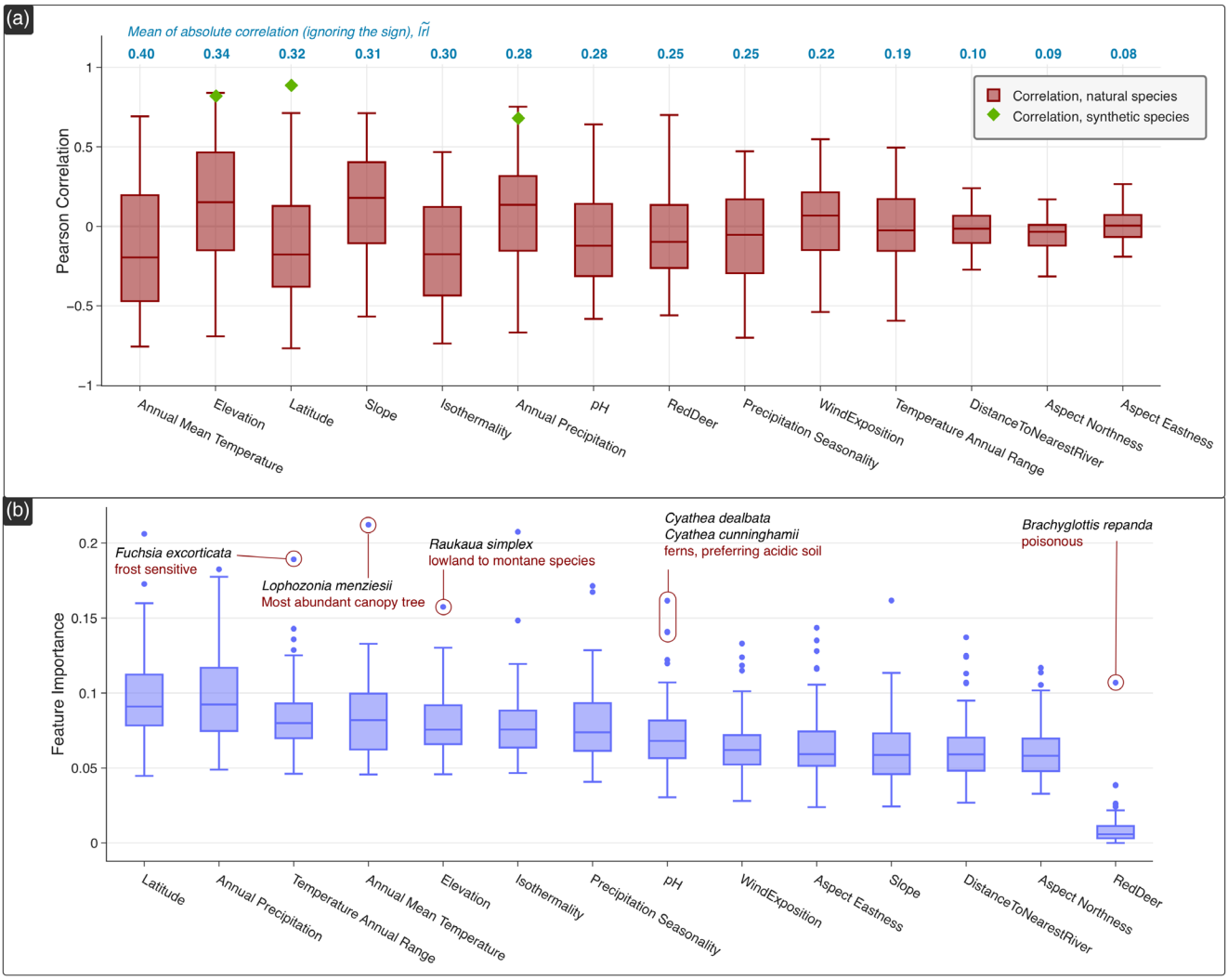

FIGURE 5 Variable importance. (a) Average Pearson's correlation of ATI and environmental variables within species' ranges (red). The average absolute values are displayed in blue text above. Correlation for synthetic species with their main drivers given as green diamonds. (b) Feature importance scores from the random forest model. Higher scores indicate a stronger reliance of the model on the variable to predict ATI. Several outlier species are highlighted.

concealed when the values are averaged. Striking examples of plant species whose abundance shifts occur strongly along a single variable are found among the outliers (highlights in Figure 5b). Notably, *Lophozonia menziesii*, possibly the most abundant tree in New Zealand, was strongly driven by annual temperature.

4 | DISCUSSION

We present the ATI, a new method to identify and map areas of change in species abundance, which draws on historical tree count data common to many biological inventories (i.e. forestry inventories). We used ATI maps to reveal 19 vulnerable species in New Zealand and their environmental pressures. Abundance gradients, derived from ATI maps, showed that species abundance of New Zealand's woody species largely matched global trends with temperature, precipitation, isothermality and pH as primary drivers, resulting in abundance shifts polewards and upslope to higher elevations (Lawlor et al., 2024; Rubenstein et al., 2023), thus validating our method. However, ATI also revealed that these mean trends poorly matched individual responses, especially for specialist species, driven by less commonly significant variables such as grazing pressure. ATI is available as a Python package, and detailed maps for this dataset are accessible on https://ati-nz-predictions-7e6f3d514735.herokuapp.com/.

4.1 | Method interpretation

ATI identifies areas of repeated positive net change in adult abundance, thereby approximating a species' demographic niche when immigration is negligible. While it explicitly models the abiotic filter, biotic interactions are implicitly captured in the data (e.g. under given conditions, a species can decline due to either abiotic or biotic filtering), thereby linking it to the fundamental niche. The

fundamental niche is defined as the species' growth rate under optimal conditions and no competition $r_0 > 0$ (Birch, 1953; Ehrlén & Morris, 2015). Although ATI does not estimate r_0 directly and includes biotic effects, an increase in adult abundance (i.e. ATI >0) is a necessary (albeit not sufficient) empirical condition for positive population growth (i.e. > 1). ATI can therefore be considered a pragmatic proxy for identifying environments with $r_0 > 0$ at landscape scales, since directly measuring r_0 is challenging, especially for long-lived trees. For instance, the COMPADRE database (Salguero-Gómez et al., 2015), which compiles demographic models globally, contains only 792 species and only one from our dataset. By contrast, the ATI estimate uses only tree-count survey pairs, which are widely available in national forest inventories. This allows ATI to complement species distribution models (Guisan & Thuiller, 2005), which do not explicitly model processes such as net population growth rate (Thuiller et al., 2013).

ATI is formulated as a binary classification model rather than a regression model. Its objective is to identify the direction of abundance change (increase vs. decrease) and to quantify the balance between positive and negative changes, which we interpret as (climate) vulnerability. The ATI score depends on the relative frequency and spatial pattern of increases and declines, not on precise estimates of absolute abundance, and is largely insensitive to absolute abundance values given their approximately normal distribution (see Section S1.8 and Figure S9). Accurate abundance modelling requires additional information on biotic interactions (Meier et al., 2010) and is context-dependent (Lynn et al., 2019), which a landscape model cannot fully capture. However, binarisation offers three key advantages. First, it enables the use of an established label noise removal framework (Brodley & Friedl, 1999; Frénay & Verleysen, 2014), which counteracts errors in forest inventory datasets estimated from 5.9% (Scott & Hallam, 2003) to 21% (Verheyen et al., 2018) (Section S2) and enables the model to capture underlying general trends with higher accuracy (Section S3.3). Second, classification models are inherently less sensitive to outliers (Loh, 2011). Third, a fivefold reduction (to $R^2 \approx 0.01$; Figure S8) in the effect of regression to the mean (RTM), where extreme initial abundance values bias the observed change in abundance (Mazalla & Diekmann, 2022), masking the relationships between environment and abundance (Section S1.7). An expansion of ATI to three classes (increase, decrease or no change) is meaningful, but requires three separate classifiers (Galar et al., 2011), increasing data requirements threefold. ATI's binary approach should therefore be viewed as a landscape-scale screening tool to identify dominant environmental drivers of abundance change and to flag species at risk, but followed by finer scale abundance analyses, such as joint species distribution models (Ovaskainen & Soininen, 2011).

Binarisation of ATI necessitated addressing areas with unchanged individual counts, resolving this via total DBH changes; however, it is problematic because DBH reflects biomass, not fitness. Long-lived adults can maintain and increase biomass despite population decline (Tilman et al., 1994). Conversely, juveniles and seed banks contribute little to DBH but increase overall fitness through recruitment. Moreover, DBH change is site-specific, influenced by factors such as soil fertility and amplified by temporal factors, including gap dynamics (Bagnato et al., 2021). However, if ATI were used to predict carbon storage, productivity or biomass dynamics, choosing DBH changes for label generation over the number of individuals would be meaningful and straightforward.

While ATI was developed on New Zealand plants, it can be applied to animals if survey protocols and detection biases are accounted for (e.g. seasonal bird migration should not count as an abundance change). A major advantage is that ATI can combine multiple abundance metrics (e.g. individual counts or detection probability changes convert equally into binary labels), solving a major issue for biodiversity tracking (Callaghan et al., 2024). Similarly to SDMs, ATI extensions would require taxon and location-specific variables (e.g. habitat structure for animals, or snow-related variables at high latitudes) (Guillera-Arroita et al., 2015), and should follow ODMAP guidelines (Zurell et al., 2020) for validation, training and documentation. We introduced a mutual information and clustering-based variable choice procedure, which incorporates training labels, is taxon-agnostic (Section S1.2) and reduces collinearity (Dormann et al., 2013). With minor adjustments, therefore, the ATI framework can be applied to other organisms and at other locations.

Our method has a few limitations that can be addressed in future implementations. First, data on land-use change would likely improve abundance predictions (Guo et al., 2018), but were unavailable for New Zealand at the time of analysis. Recently developed global land-use datasets (e.g. Woodman et al., 2026) provide a clear next step for improving ATI predictions. Our method does not account for species interactions or density dependence (Chesson, 2000), and likely removes their effects in the data cleaning step. Density dependence strongly influences abundance distributions (Ehrlén & Morris, 2015) and, as we demonstrate for inference, can be accounted for in ATI by including abundance as a predictive variable, improving model performance (Figure S12A). For the prediction case, it would need to be estimated or measured. Second, abundance shifts result from a change in fitness, mediated by a species' traits (Funk et al., 2017; Laughlin, 2023). Incorporating trait data might, therefore, allow us to unify species-specific ATI models into a single model, vastly expanding the training dataset and enabling more complex models that can infer successful trait combinations (i.e. functional strategies). Finally, while ATI successfully recovers abundance gradients for synthetic species (Section S3.4), full ecological validation at the landscape scale will require future studies using independent or targeted datasets.

4.2 | Ecological results

Our results align New Zealand's flora with global trends of abundance shifts towards the poles and to higher, cooler elevations (Lenoir et al., 2020; Parmesan & Yohe, 2003; Figure 3). However, temperature and elevation had only a modest twofold difference in feature importance to the least influential variables (Figure 5b). These variables contributed to within-range biodiversity rearrangement,

especially for specialist species (outliers in Figure 5b), pointing to their importance in predicting abundance shifts and consequent range shifts (Franklin, 2023; Howard et al., 2014). The presence of multiple interacting abundance gradients is further exemplified by comparing the lower prediction accuracy of real-world species (average AUC = 0.62) to that of synthetic species (driven by a single variable, AUC >0.85; Section S3.4, Figure 5a). These findings illustrate ATI's advantage in capturing the complex interplay of a wide array of environmental drivers within a species' range, addressing limitations of previous work, overlooking within-range abundance dynamics (Rubenstein et al., 2023; Taheri et al., 2021).

Abundance gradients for all species were predominantly distributed along an axis from stress tolerance (PC1 in Figure 4d) to avoidance. The ability to move (i.e. avoid stress) or persist (i.e. tolerate stress) determines a species' demographic success (Lenoir & Svenning, 2015). However, environmental conditions translate into stress differently for each species (Lichtenthaler, 1998), and thus, predicting abundance changes requires consideration of what constitutes stress to each species within the studied habitat. For example, the toxic *Brachyglottis repanda* has a competitive advantage under grazing pressure (Mortimer & White, 1967), and showed the strongest feature importance score for this variable (Figure 5b). This species-specificity is illustrated by the majority of abundance gradients lying outside the 1σ margin around the mean gradient (Figure 4a–c), in other words, the mean response of all species is not a common response of any species. This illustrates that a better understanding of biodiversity rearrangement needs to consider individual plant stressors caused by a diverse range of factors.

Vulnerability assessments for individual species at a landscape scale are often costly, time-consuming, and dependent on limited expert opinions (Ackerly et al., 2010) and might not reflect species' shrinking ranges (Goury et al., 2025). Recently developed climate-based methods broadly assess biodiversity risk but sacrifice precision (Klausmeyer et al., 2011). ATI, on the other hand, enables broad-scale climate vulnerability assessments for individual species by identifying species with predominantly declining abundances. An important limitation of this metric is that it does not account for aspects of vulnerability beyond climate, such as introduced diseases, dispersal limitation, or habitat destruction and fragmentation, unless they are included as predictive variables (e.g. deer presence in our data). We identified 19 such species across New Zealand whose vulnerability is driven by climatic variability, particularly temperature range and precipitation seasonality. Despite mean annual temperature (MAT) being more important collectively (Figure 5a), it was not of primary importance to any of the vulnerable species (Figure 2b). This aligns with experimental evidence that limited adaptive phenotypic plasticity to climatic variability, rather than tolerance to mean climate, often determines population persistence under changing conditions (Reyer et al., 2013; Scheepens et al., 2018), highlighting that increasing fluctuations may pose a stronger risk than shifts in climatic means. Alarmingly, two of the most vulnerable species (*Metrosideros diffusa* and *Metrosideros fulgens*) belong to the Myrtaceae family, which is susceptible to the recently introduced invasive fungal pathogen *Austropuccinia psidii* (myrtle rust) (Toome-Heller et al., 2020). Given that only 2 years in our dataset overlap with the presence of myrtle rust, this may reflect interacting pressures of climate variability and disease, highlighting these species as priorities for closer monitoring under ongoing environmental change.

5 | CONCLUSION

Our study underscores the necessity of examining within-range abundance changes to understand forest plant species' responses to recent climate change. The ATI leverages freely available forest inventory data to identify spatially explicit changes in species abundance and reveals that species respond individually rather than following mean trends, often as a function of unstable environmental conditions. Moreover, the focus on abundance ties the model outputs closer to niche theory and enhances our ability to identify vulnerable species and the specific factors contributing to their decline. By using ATI alongside species distribution models, we can refine ecological predictions and inform conservation strategies more effectively. ATI is easily expanded to other organisms and locations, provided abundance changes can be detected reliably. A Python package for ATI is available, and an interactive website (https://ati-nz-predictions-7e6f3d514735.herokuapp.com/) showcases detailed results to foster broader familiarity with ATI.

AUTHOR CONTRIBUTIONS

Ilya Shabanov and Julie R. Deslippe conceived the initial ideas, and all authors designed the methodology; Ilya Shabanov compiled the data; Ilya Shabanov and Andrew Lensen analysed the data; Ilya Shabanov and Julie R. Deslippe led the writing of the manuscript. All authors contributed critically to the drafts and gave final approval for publication.

ACKNOWLEDGEMENTS

We acknowledge Jonathan Lenoir and two anonymous reviewers for valuable feedback on an earlier version of this manuscript. Bioprotection Aotearoa - Centre of Research Excellence, funded by the New Zealand Tertiary Education Commission Centres of Research Excellence Fund (E4050-3443). Open access publishing facilitated by Victoria University of Wellington, as part of the Wiley - Victoria University of Wellington agreement via the Council of Australasian University Librarians

CONFLICT OF INTEREST STATEMENT

The authors declare no conflicts of interest.

PEER REVIEW

The peer review history for this article is available at https://www.webofscience.com/api/gateway/wos/peer-review/10.1111/1365-2745.70344.

DATA AVAILABILITY STATEMENT

Range shift predictions, directions and variable importance values presented in this paper can be interactively explored at https://ati-nz-predictions-7e6f3d514735.herokuapp.com/ for most species, environmental variables, datasets and variable sets. Trained models and the Python code repository for data preprocessing, model training and generating synthetic species of this study are openly available from Zenodo at https://doi.org/10.5281/ZENODO.12703232 (Shabanov et al., 2026). The raw forest inventory data from New Zealand's National Vegetation Survey (NVS) remains owned by NVS, and the meta-data from these sites is not public. Please contact NVS (https://nvs.landcareresearch.co.nz/) for permission to use their data, which is generally available on a per-project basis. This study's climate data is available at https://essd.copernicus.org/articles/14/2817/2022/essd-14-2817-2022-discussion.html, reference (Etherington et al., 2022). Environmental data (e.g. elevation, slope, edaphic factors) are openly available at https://datastore.landcaresearch.co.nz/dataset/nzenvds, reference (McCarthy et al., 2021). Data on the presence of possums, red deer and rats are openly available at https://data.mfe.govt.nz/x/NDiRh9, https://data.mfe.govt.nz/x/dyKrZA and https://data.mfe.govt.nz/x/zbW9de, respectively.

ORCID

Ilya Shabanov https://orcid.org/0000-0003-0107-5365
Andrew Lensen https://orcid.org/0000-0003-1269-4751
Jonathan Tonkin https://orcid.org/0000-0002-6053-291X
Julie R. Deslippe https://orcid.org/0000-0003-0511-9062

REFERENCES

Ackerly, D. D., Loarie, S. R., Cornwell, W. K., Weiss, S. B., Hamilton, H., Branciforte, R., & Kraft, N. J. B. (2010). The geography of climate change: Implications for conservation biogeography: Geography of climate change. *Diversity and Distributions*, *16*(3), 476–487. https://doi.org/10.1111/j.1472-4642.2010.00654.x

Araújo, M. B., Pearson, R. G., Thuiller, W., & Erhard, M. (2005). Validation of species–climate impact models under climate change. *Global Change Biology*, *11*(9), 1504–1513. https://doi.org/10.1111/j.1365-2486.2005.01000.x

Bagnato, S., Marziliano, P. A., Sidari, M., Mallamaci, C., Marra, F., & Muscolo, A. (2021). Effects of gap size and cardinal directions on natural regeneration, growth dynamics of trees outside the gaps and soil properties in European beech forests of southern Italy. *Forests*, *12*(11), 1563. https://doi.org/10.3390/f12111563

Bartley, M. L., Hanks, E. M., Schliep, E. M., Soranno, P. A., & Wagner, T. (2019). Identifying and characterizing extrapolation in multivariate response data. *PLoS One*, *14*(12), e0225715. https://doi.org/10.1371/journal.pone.0225715

Beckage, B., Osborne, B., Gavin, D. G., Pucko, C., Siccama, T., & Perkins, T. (2008). A rapid upward shift of a forest ecotone during 40 years of warming in the Green Mountains of Vermont. *Proceedings of the National Academy of Sciences of the United States of America*, *105*(11), 4197–4202. https://doi.org/10.1073/pnas.0708921105

Birch, L. C. (1953). EXPERIMENTAL BACKGROUND TO THE STUDY OF THE DISTRIBUTION AND ABUNDANCE OF INSECTS: III. THE relation between innate capacity for increase and survival of different species of beetles living together on THE same food. *Evolution; International Journal of Organic Evolution*, *7*(2), 136–144. https://doi.org/10.1111/j.1558-5646.1953.tb00072.x

Breiman, L. (2001). Random forests. *Machine Learning*, *45*(1), 5–32. https://doi.org/10.1023/A:1010933404324

Breshears, D. D., Huxman, T. E., Adams, H. D., Zou, C. B., & Davison, J. E. (2008). Vegetation synchronously leans upslope as climate warms. *Proceedings of the National Academy of Sciences of the United States of America*, *105*(33), 11591–11592. https://doi.org/10.1073/pnas.0806579105

Brodley, C. E., & Friedl, M. A. (1999). Identifying mislabeled training data. *Journal of Artificial Intelligence Research*, *11*, 131–167. https://doi.org/10.1613/jair.606

Callaghan, C. T., Santini, L., Spake, R., & Bowler, D. E. (2024). Population abundance estimates in conservation and biodiversity research. *Trends in Ecology & Evolution*, *39*(6), 515–523. https://doi.org/10.1016/j.tree.2024.01.012

Caswell, H. (2006). Matrix population models. In *Encyclopedia of environmetrics*. John Wiley & Sons, Ltd. https://onlinelibrary.wiley.com/doi/abs/10.1002/9780470057339.vam006m

Chesson, P. (2000). Mechanisms of maintenance of species diversity. *Annual Review of Ecology, Evolution, and Systematics*, *31*, 343–366. https://doi.org/10.1146/annurev.ecolsys.31.1.343

Chirici, G., McRoberts, R. E., Winter, S., Bertini, R., Brändli, U.-B., Asensio, I. A., Bastrup-Birk, A., Rondeux, J., Barsoum, N., & Marchetti, M. (2012). National forest inventory contributions to forest biodiversity monitoring. *Forest Science*, *58*(3), 257–268. https://doi.org/10.5849/forsci.12-003

Connolly, S. R., Keith, S. A., Colwell, R. K., & Rahbek, C. (2017). Process, mechanism, and modeling in macroecology. *Trends in Ecology & Evolution*, *32*(11), 835–844. https://doi.org/10.1016/j.tree.2017.08.011

Crimmins, S. M., Dobrowski, S. Z., Greenberg, J. A., Abatzoglou, J. T., & Mynsberge, A. R. (2011). Changes in climatic water balance drive downhill shifts in plant species' optimum elevations. *Science*, *331*(6015), 324–327. https://doi.org/10.1126/science.1199040

Department of Conservation. (2015a). *Distribution of possums 2002–2014 [map]*. New Zealand's Environmental Reporting Series: The Ministry for the Environment and Statistics New Zealand. https://data.mfe.govt.nz/x/NDiRh9

Department of Conservation. (2015b). *Distribution of rats 2002–2014 [map]*. New Zealand's Environmental Reporting Series: The Ministry for the Environment and Statistics New Zealand. https://data.mfe.govt.nz/x/zbW9de

Department of Conservation. (2015c). *Distribution of red deer 2002–2014 [map]*. New Zealand's Environmental Reporting Series: The Ministry for the Environment and Statistics New Zealand. https://data.mfe.govt.nz/x/dyKrZA

Diamond, S. E. (2018). Contemporary climate-driven range shifts: Putting evolution back on the table. *Functional Ecology*, *32*(7), 1652–1665. https://doi.org/10.1111/1365-2435.13095

Doak, D. F., & Morris, W. F. (2010). Demographic compensation and tipping points in climate-induced range shifts. *Nature*, *467*(7318), 959–962. https://doi.org/10.1038/nature09439

Dormann, C. F., Elith, J., Bacher, S., Buchmann, C., Carl, G., Carré, G., Marquéz, J. R. G., Gruber, B., Lafourcade, B., Leitão, P. J., Münkemüller, T., McClean, C., Osborne, P. E., Reineking, B., Schröder, B., Skidmore, A. K., Zurell, D., & Lautenbach, S. (2013). Collinearity: A review of methods to deal with it and a simulation study evaluating their performance. *Ecography*, *36*(1), 27–46. https://doi.org/10.1111/j.1600-0587.2012.07348.x

Dormann, C. F., Schymanski, S. J., Cabral, J., Chuine, I., Graham, C., Hartig, F., Kearney, M., Morin, X., Römermann, C., Schröder, B., & Singer, A. (2012). Correlation and process in species distribution models: Bridging a dichotomy: Bridging the correlation-process dichotomy. *Journal of Biogeography*, *39*(12), 2119–2131. https://doi.org/10.1111/j.1365-2699.2011.02659.x

Ehrlén, J., & Morris, W. F. (2015). Predicting changes in the distribution and abundance of species under environmental change. *Ecology Letters*, *18*, 303–314. https://doi.org/10.1111/ELE.12410

Etherington, T. R., Perry, G. L. W., & Wilmshurst, J. M. (2022). HOTRUNZ: An open-access 1 km resolution monthly 1910–2019 time series of interpolated temperature and rainfall grids with associated uncertainty for New Zealand. *Earth System Science Data*, *14*(6), 2817–2832. https://doi.org/10.5194/essd-14-2817-2022

Ewers, R. M., Kliskey, A. D., Walker, S., Rutledge, D., Harding, J. S., & Didham, R. K. (2006). Past and future trajectories of forest loss in New Zealand. *Biological Conservation*, *133*(3), 312–325. https://doi.org/10.1016/j.biocon.2006.06.018

Fawcett, T. (2006). An introduction to ROC analysis. *Pattern Recognition Letters*, *27*(8), 861–874. https://doi.org/10.1016/j.patrec.2005.10.010

Fei, S., Desprez, J. M., Potter, K. M., Jo, I., Knott, J. A., & Oswalt, C. M. (2017). Divergence of species responses to climate change. *Science Advances*, *3*(5), e1603055. https://doi.org/10.1126/sciadv.1603055

Fischer, H. S. (2015). On the combination of species cover values from different vegetation layers. *Applied Vegetation Science*, *18*(1), 169–170. https://doi.org/10.1111/avsc.12130

Foden, W. B., Young, B. E., Akçakaya, H. R., Garcia, R. A., Hoffmann, A. A., Stein, B. A., Thomas, C. D., Wheatley, C. J., Bickford, D., Carr, J. A., Hole, D. G., Martin, T. G., Pacifici, M., Pearce-Higgins, J. W., Platts, P. J., Visconti, P., Watson, J. E. M., & Huntley, B. (2019). Climate change vulnerability assessment of species. *Wiley Interdisciplinary Reviews: Climate Change*, *10*(1), e551. https://doi.org/10.1002/wcc.551

Forsyth, D., Wilmshurst, J., Allen, R., & Coomes, D. (2010). Impacts of introduced deer and extinct moa on New Zealand ecosystems. *New Zealand Journal of Ecology*, *34*(1), 48–65.

Franklin, J. (2023). Species distribution modelling supports the study of past, present and future biogeographies. *Journal of Biogeography*, *50*(9), 1533–1545. https://doi.org/10.1111/jbi.14617

Frénay, B., & Verleysen, M. (2014). Classification in the presence of label noise: A survey. *IEEE Transactions on Neural Networks and Learning Systems*, *25*(5), 845–869. https://doi.org/10.1109/TNNLS.2013.2292894

Funk, J. L., Larson, J. E., Ames, G. M., Butterfield, B. J., Cavender-Bares, J., Firn, J., Laughlin, D. C., Sutton-Grier, A. E., Williams, L., & Wright, J. (2017). Revisiting the holy grail: Using plant functional traits to understand ecological processes. *Biological Reviews of the Cambridge Philosophical Society*, *92*(2), 1156–1173. https://doi.org/10.1111/brv.12275

Galar, M., Fernández, A., Barrenechea, E., Bustince, H., & Herrera, F. (2011). An overview of ensemble methods for binary classifiers in multi-class problems: Experimental study on one-vs-one and one-vs-all schemes. *Pattern Recognition*, *44*(8), 1761–1776. https://doi.org/10.1016/j.patcog.2011.01.017

Gougherty, A. V., Prasad, A. M., Peters, M. P., Matthews, S. N., & Adams, B. T. (2024). Climate change and the emergence of no-analog forest assemblages in North America. *Global Change Biology*, *30*(12), e17605. https://doi.org/10.1111/gcb.17605

Goury, R., Thuiller, W., Abdulhak, S., Pache, G., Van Es, J., Bowler, D. E., Renaud, J., Violle, C., & Münkemüller, T. (2025). Recent vegetation shifts in the French Alps with winners outnumbering losers. *The Journal of Ecology*, *113*(11), 3275–3292. https://doi.org/10.1111/1365-2745.70159

Guillera-Arroita, G., Lahoz-Monfort, J. J., Elith, J., Gordon, A., Kujala, H., Lentini, P. E., McCarthy, M. A., Tingley, R., & Wintle, B. A. (2015). Is my species distribution model fit for purpose? Matching data and models to applications: Matching distribution models to applications. *Global Ecology and Biogeography: A Journal of Macroecology*, *24*(3), 276–292. https://doi.org/10.1111/geb.12268

Guisan, A., & Thuiller, W. (2005). Predicting species distribution: Offering more than simple habitat models. *Ecology Letters*, *8*(9), 993–1009. https://doi.org/10.1111/j.1461-0248.2005.00792.x

Guo, F., Lenoir, J., & Bonebrake, T. C. (2018). Land-use change interacts with climate to determine elevational species redistribution. *Nature Communications*, *9*(1), 1315. https://doi.org/10.1038/s41467-018-03786-9

Heino, M., Kummu, M., Makkonen, M., Mulligan, M., Verburg, P. H., Jalava, M., & Räsänen, T. A. (2015). Forest loss in protected areas and intact forest landscapes: A global analysis. *PLoS One*, *10*(10), e0138918. https://doi.org/10.1371/journal.pone.0138918

Howard, C., Stephens, P. A., Pearce-Higgins, J. W., Gregory, R. D., & Willis, S. G. (2014). Improving species distribution models: The value of data on abundance. *Methods in Ecology and Evolution*, *5*(6), 506–513. https://doi.org/10.1111/2041-210X.12184

Hurst, J. M. (2022). *The Recce method for describing New Zealand vegetation-field manual*. Manaaki Whenua Press. https://doi.org/10.7931/P48H-ZB65

Jakoby, O., Lischke, H., & Wermelinger, B. (2019). Climate change alters elevational phenology patterns of the European spruce bark beetle (*Ips typographus*). *Global Change Biology*, *25*(12), 4048–4063. https://doi.org/10.1111/gcb.14766

Jia, S., Wang, X., Yuan, Z., Lin, F., Ye, J., Hao, Z., & Luskin, M. S. (2018). Global signal of top-down control of terrestrial plant communities by herbivores. *Proceedings of the National Academy of Sciences of the United States of America*, *115*(24), 6237–6242. https://doi.org/10.1073/pnas.1707984115

Johnston, A., Fink, D., Reynolds, M. D., Hochachka, W. M., Sullivan, B. L., Bruns, N. E., Hallstein, E., Merrifield, M. S., Matsumoto, S., & Kelling, S. (2015). Abundance models improve spatial and temporal prioritization of conservation resources. *Ecological Applications: A Publication of the Ecological Society of America*, *25*(7), 1749–1756. https://doi.org/10.1890/14-1826.1

Klausmeyer, K. R., Shaw, M. R., MacKenzie, J. B., & Cameron, D. R. (2011). Landscape-scale indicators of biodiversity's vulnerability to climate change. *Ecosphere (Washington, D.C.)*, *2*(8), art88. https://doi.org/10.1890/es11-00044.1

Laughlin, D. C. (2023). *Plant strategies: The demographic consequences of functional traits in changing environments*. Oxford University Press. https://play.google.com/store/books/details?id=0aakzwEACAAJ

Lawlor, J. A., Comte, L., Grenouillet, G., Lenoir, J., Baecher, J. A., Bandara, R. M. W. J., Bertrand, R., Chen, I.-C., Diamond, S. E., Lancaster, L. T., Moore, N., Murienne, J., Oliveira, B. F., Pecl, G. T., Pinsky, M. L., Rolland, J., Rubenstein, M., Scheffers, B. R., Thompson, L. M., … Sunday, J. (2024). Mechanisms, detection and impacts of species redistributions under climate change. *Nature Reviews Earth and Environment*, *5*(5), 351–368. https://doi.org/10.1038/s43017-024-00527-z

Lee-Yaw, J. A., McCune, J. L., Pironon, S., & Sheth, S. N. (2022). Species distribution models rarely predict the biology of real populations. *Ecography*, *2022*(6), e05877. https://doi.org/10.1111/ecog.05877

Lenoir, J., Bertrand, R., Comte, L., Bourgeaud, L., Hattab, T., Murienne, J., & Grenouillet, G. (2020). Species better track climate warming in the oceans than on land. *Nature Ecology & Evolution*, *4*, 1044–1059. https://doi.org/10.1038/S41559-020-1198-2

Lenoir, J., Gégout, J.-C., Guisan, A., Vittoz, P., Wohlgemuth, T., Zimmermann, N. E., Dullinger, S., Pauli, H., Willner, W., & Svenning, J.-C. (2010). Going against the flow: Potential mechanisms for unexpected downslope range shifts in a warming climate. *Ecography*, *33*(2), 295–303. https://doi.org/10.1111/j.1600-0587.2010.06279.x

Lenoir, J., Gégout, J.-C., Pierrat, J.-C., Bontemps, J.-D., & Dhôte, J.-F. (2009). Differences between tree species seedling and adult altitudinal distribution in mountain forests during the recent warm period (1986-2006). *Ecography*, *32*(5), 765–777. https://doi.org/10.1111/j.1600-0587.2009.05791.x

Lenoir, J., & Svenning, J.-C. (2015). Climate-related range shifts—A global multidimensional synthesis and new research directions. *Ecography*, *38*(1), 15–28. https://doi.org/10.1111/ecog.00967

Lichtenthaler, H. K. (1998). The stress concept in plants: An introduction. *Annals of the New York Academy of Sciences*, *851*, 187–198. https://doi.org/10.1111/j.1749-6632.1998.tb08993.x

Loh, W.-Y. (2011). Classification and regression trees: Classification and regression trees. *Wiley Interdisciplinary Reviews: Data Mining and Knowledge Discovery*, *1*(1), 14–23. https://doi.org/10.1002/widm.8

Louthan, A. M., Doak, D. F., & Angert, A. L. (2015). Where and when do species interactions set range limits? *Trends in Ecology & Evolution*, *30*(12), 780–792. https://doi.org/10.1016/j.tree.2015.09.011

Lynn, J. S., Kazenel, M. R., Kivlin, S. N., & Rudgers, J. A. (2019). Context-dependent biotic interactions control plant abundance across altitudinal environmental gradients. *Ecography*, *42*(9), 1600–1612. https://doi.org/10.1111/ecog.04421

Lynn, J. S., Klanderud, K., Telford, R. J., Goldberg, D. E., & Vandvik, V. (2021). Macroecological context predicts species' responses to climate warming. *Global Change Biology*, *27*(10), 2088–2101. https://doi.org/10.1111/gcb.15532

Mazalla, L., & Diekmann, M. (2022). Regression to the mean in vegetation science. *Journal of Vegetation Science: Official Organ of the International Association for Vegetation Science*, *33*(2), e13117. https://doi.org/10.1111/jvs.13117

McCarthy, J., Leathwick, J., Roudier, P., Barringer, J., Etherington, T., Morgan, F., Odgers, N., Price, R., Wiser, S., & Richardson, S. (2021). New Zealand Environmental Data Stack (NZEnvDS): A standardised collection of spatial layers for environmental modelling and site characterisation. *New Zealand Journal of Ecology*. https://doi.org/10.20417/nzjecol.45.31

Meier, E. S., Kienast, F., Pearman, P. B., Svenning, J.-C., Thuiller, W., Araújo, M. B., Guisan, A., & Zimmermann, N. E. (2010). Biotic and abiotic variables show little redundancy in explaining tree species distributions. *Ecography*, *33*(6), 1038–1048. https://doi.org/10.1111/j.1600-0587.2010.06229.x

Molnar, C. (2022). *Interpretable machine learning. A guide for making black box models explainable* (2nd ed.). https://christophm.github.io/interpretable-ml-book

Mortimer, P. H., & White, E. P. (1967). Hepatotoxic substance in *Brachyglottis repanda*. *Nature*, *214*(5094), 1255–1256. https://doi.org/10.1038/2141255a0

Murray, B. G., & de Lange, P. J. (2011). Chromosomes and evolution in New Zealand endemic angiosperms and gymnosperms. In D. Bramwell & J. Caujape-castells (Eds.), *The biology of Island floras* (pp. 265–283). Cambridge University Press. https://doi.org/10.1017/cbo9780511844270.012

O'Donnel, M. S., & Ignizio, D. A. (2012). *Bioclimatic predictors for supporting ecological applications in the conterminous United States (No. 691)*. U.S. Geological Survey. https://pubs.usgs.gov/publication/ds691

Ovaskainen, O., & Soininen, J. (2011). Making more out of sparse data: Hierarchical modeling of species communities. *Ecology*, *92*(2), 289–295. https://doi.org/10.1890/10-1251.1

Owens, H. L., Campbell, L. P., Dornak, L. L., Saupe, E. E., Barve, N., Soberón, J., Ingenloff, K., Lira-Noriega, A., Hensz, C. M., Myers, C. E., & Peterson, A. T. (2013). Constraints on interpretation of ecological niche models by limited environmental ranges on calibration areas. *Ecological Modelling*, *263*, 10–18. https://doi.org/10.1016/j.ecolmodel.2013.04.011

Pagel, J., Treurnicht, M., Bond, W. J., Kraaij, T., Nottebrock, H., Schutte-Vlok, A., Tonnabel, J., Esler, K. J., & Schurr, F. M. (2020). Mismatches between demographic niches and geographic distributions are strongest in poorly dispersed and highly persistent plant species. *Proceedings of the National Academy of Sciences of the United States of America*, *117*(7), 3663–3669. https://doi.org/10.1073/pnas.1908684117

Parmesan, C., & Yohe, G. (2003). A globally coherent fingerprint of climate change impacts across natural systems. *Nature*, *421*(6918), 37–42. https://doi.org/10.1038/nature01286

Pearson, R. G., Raxworthy, C. J., Nakamura, M., & Townsend Peterson, A. (2007). ORIGINAL ARTICLE: Predicting species distributions from small numbers of occurrence records: A test case using cryptic geckos in Madagascar: Predicting species distributions with low sample sizes. *Journal of Biogeography*, *34*(1), 102–117. https://doi.org/10.1111/j.1365-2699.2006.01594.x

Pedregosa, F., Varoquaux, G., Gramfort, A., Michel, V., Thirion, B., Grisel, O., Blondel, M., Prettenhofer, P., Weiss, R., Dubourg, V., Vanderplas, J., Passos, A., Cournapeau, D., Brucher, M., Perrot, M., & Duchesnay, E. (2011). Scikit-learn: Machine learning in python. *Journal of Machine Learning Research*, *12*, 2825–2830.

Rapacciuolo, G., Maher, S. P., Schneider, A. C., Hammond, T. T., Jabis, M. D., Walsh, R. E., Iknayan, K. J., Walden, G. K., Oldfather, M. F., Ackerly, D. D., & Beissinger, S. R. (2014). Beyond a warming fingerprint: Individualistic biogeographic responses to heterogeneous climate change in California. *Global Change Biology*, *20*(9), 2841–2855. https://doi.org/10.1111/gcb.12638

Reyer, C. P. O., Leuzinger, S., Rammig, A., Wolf, A., Bartholomeus, R. P., Bonfante, A., de Lorenzi, F., Dury, M., Gloning, P., Abou Jaoudé, R., Klein, T., Kuster, T. M., Martins, M., Niedrist, G., Riccardi, M., Wohlfahrt, G., de Angelis, P., de Dato, G., François, L., … Pereira, M. (2013). A plant's perspective of extremes: Terrestrial plant responses to changing climatic variability. *Global Change Biology*, *19*(1), 75–89. https://doi.org/10.1111/gcb.12023

Rubenstein, M. A., Weiskopf, S. R., Bertrand, R., Carter, S. L., Comte, L., Eaton, M. J., Johnson, C. G., Lenoir, J., Lynch, A. J., Miller, B. W., Morelli, T. L., Rodriguez, M. A., Terando, A., & Thompson, L. M. (2023). Climate change and the global redistribution of biodiversity: Substantial variation in empirical support for expected range shifts. *Environmental Evidence*, *12*(1), 1–21. https://doi.org/10.1186/s13750-023-00296-0

Salguero-Gómez, R., Jones, O. R., Archer, C. R., Buckley, Y. M., Che-Castaldo, J., Caswell, H., Hodgson, D., Scheuerlein, A., Conde, D. A., Brinks, E., de Buhr, H., Farack, C., Gottschalk, F., Hartmann, A., Henning, A., Hoppe, G., Römer, G., Runge, J., Ruoff, T., … Vaupel, J. W. (2015). The compadrePlant matrix database: An open online repository for plant demography. *The Journal of Ecology*, *103*(1), 202–218. https://doi.org/10.1111/1365-2745.12334

Scheepens, J. F., Deng, Y., & Bossdorf, O. (2018). Phenotypic plasticity in response to temperature fluctuations is genetically variable, and relates to climatic variability of origin, in Arabidopsis thaliana. *AoB Plants*, *10*(4), ly043. https://doi.org/10.1093/aobpla/ply043

Scott, W. A., & Hallam, C. J. (2003). Assessing species misidentification rates through quality assurance of vegetation monitoring. *Plant Ecology*, *165*(1), 101–115. https://doi.org/10.1023/a:1021441331839

Shabanov, I., Deslippe, J., Lensen, A., & Tonkin, J. (2026). *Abundance trend indicator-models, prediction, stacked environmental data and training set similarity* [dataset]. *Zenodo*. https://doi.org/10.5281/ZENODO.12703232

Stephenson, N. (1998). Actual evapotranspiration and deficit: Biologically meaningful correlates of vegetation distribution across spatial scales. *Journal of Biogeography*, *25*(5), 855–870. https://doi.org/10.1046/j.1365-2699.1998.00233.x

Taheri, S., Naimi, B., Rahbek, C., & Araújo, M. B. (2021). Improvements in reports of species redistribution under climate change are required. *Science Advances*, *7*(15), eabe1110. https://doi.org/10.1126/sciadv.abe1110

Thompson, I. D., Maher, S. C., Rouillard, D. P., Fryxell, J. M., & Baker, J. A. (2007). Accuracy of forest inventory mapping: Some implications for boreal forest management. *Forest Ecology and Management*, *252*(1), 208–221. https://doi.org/10.1016/j.foreco.2007.06.033

Thuiller, W., Münkemüller, T., Lavergne, S., Mouillot, D., Mouquet, N., Schiffers, K., & Gravel, D. (2013). A road map for integrating eco-evolutionary processes into biodiversity models. *Ecology Letters*, *16*(Suppl 1), 94–105. https://doi.org/10.1111/ele.12104

Tilman, D., May, R. M., Lehman, C. L., & Nowak, M. A. (1994). Habitat destruction and the extinction debt. *Nature*, *371*(6492), 65–66. https://doi.org/10.1038/371065a0

Tomppo, E., Gschwantner, T., Lawrence, M., & McRoberts, R. E. (2009). *National forest inventories: Pathways for common reporting [PDF]*. Springer. https://doi.org/10.1007/978-90-481-3233-1

Toome-Heller, M., Ho, W. W. H., Ganley, R. J., Elliott, C. E. A., Quinn, B., Pearson, H. G., & Alexander, B. J. R. (2020). Chasing myrtle rust in New Zealand: Host range and distribution over the first year after

invasion. *Australasian Plant Pathology*, *49*(3), 221–230. https://doi.org/10.1007/s13313-020-00694-9

Verheyen, K., Bažány, M., Chećko, E., Chudomelová, M., Closset-Kopp, D., Czortek, P., Decocq, G., De Frenne, P., De Keersmaeker, L., Enríquez García, C., Fabšičová, M., Grytnes, J.-A., Hederová, L., Hédl, R., Heinken, T., Schei, F. H., Horváth, S., Jaroszewicz, B., Jermakowicz, E., … Baeten, L. (2018). Observer and relocation errors matter in re-surveys of historical vegetation plots. *Journal of Vegetation Science: Official Organ of the International Association for Vegetation Science*, *29*(5), 812–823. https://doi.org/10.1111/jvs.12673

Villellas, J., Doak, D. F., García, M. B., & Morris, W. F. (2015). Demographic compensation among populations: What is it, how does it arise and what are its implications? *Ecology Letters*, *18*(11), 1139–1152. https://doi.org/10.1111/ele.12505

Williams, J. W., Jackson, S. T., & Kutzbach, J. E. (2007). Projected distributions of novel and disappearing climates by 2100 AD. *Proceedings of the National Academy of Sciences of the United States of America*, *104*(14), 5738–5742. https://doi.org/10.1073/pnas.0606292104

Wiser, S. K., Bellingham, P. J., & Burrows, L. E. (2001). Managing biodiversity information: Development of New Zealand's National Vegetation Survey databank. *New Zealand Journal of Ecology*, *25*(2), 1–17.

Wisz, M. S., Hijmans, R. J., Li, J., Peterson, A. T., Graham, C. H., Guisan, A., & NCEAS Predicting Species Distributions Working Group†. (2008). Effects of sample size on the performance of species distribution models. *Diversity and Distributions*, *14*(5), 763–773. https://doi.org/10.1111/j.1472-4642.2008.00482.x

Woodall, C. W., Oswalt, C. M., Westfall, J. A., Perry, C. H., Nelson, M. D., & Finley, A. O. (2009). An indicator of tree migration in forests of the eastern United States. *Forest Ecology and Management*, *257*(5), 1434–1444. https://doi.org/10.1016/j.foreco.2008.12.013

Woodman, T. L., Arendarczyk, B., Winkler, K., Henry, R. C., Eigenbrod, F., Burslem, D. F. R. P., Alexander, P., & Travis, J. M. J. (2026). High-resolution land-use maps from 1960 to 2100. *One Earth (Cambridge, Mass.)*, *9*(2), 101525. https://doi.org/10.1016/j.oneear.2025.101525

Wyse, S., Wilmshurst, J., Burns, B., & Perry, G. (2018). New Zealand forest dynamics: A review of past and present vegetation responses to disturbance, and development of conceptual forest models. *New Zealand Journal of Ecology*, *42*(2), 87–106. https://doi.org/10.20417/nzjecol.42.18

Zotov, V. D. (1938). *An outline of the vegetation and Flora of the Tararua Mountains*. Transactions and Proceedings of the NZ Institute.

Zurell, D., Franklin, J., König, C., Bouchet, P. J., Dormann, C. F., Elith, J., Fandos, G., Feng, X., Guillera-Arroita, G., Guisan, A., Lahoz-Monfort, J. J., Leitão, P. J., Park, D. S., Peterson, A. T., Rapacciuolo, G., Schmatz, D. R., Schröder, B., Serra-Diaz, J. M., Thuiller, W., … Merow, C. (2020). A standard protocol for reporting species distribution models. *Ecography*, *43*, 1261–1277. https://doi.org/10.1111/ECOG.04960

SUPPORTING INFORMATION

Additional supporting information can be found online in the Supporting Information section at the end of this article.

Figure S1. Data statistics for the Abundance and DBH dataset containing 86 species with sufficient data and covering 75.59% of the forest canopy. A: Number of observations by species and their cumulative canopy cover, ordered by the number of observations. B: The distribution of the classes shows a slight class imbalance. C: Number of measurements by time between them. Each measurement is a plot that has been surveyed twice, with a certain number of years between measurements. D: The average number of plot remeasurements. Most plots have only been measured twice, yielding a single observation for the occurring species.

Figure S2. Dimensionality reduction used to generate the Reduced Dataset. A: Result of the hierarchical clustering procedure with distance metric set to the absolute value of the correlation between values and Ward's linkage. Clusters below 0.5 are highlighted in different colours. The number behind each variable is the mean mutual information value. For readability, it is normalised such that all values sum up to 100. B: Histogram of pairwise correlations between the variables in the Full and Reduced datasets, respectively. Showing a reduction of highly correlated variables. C: Mutual information of the variable and the training label (increase/decrease) across all species. Lower numbers indicate lower dependence of the target labels on the variable.

Table S1. List of variables included in the Reduced dataset. Lists the 18 clusters from Figure S2 along with their mutual information values (normalised so that they sum up to 100). From each cluster, one (in some cases none) variable is included, and the reason for including and excluding is given in the 'Comment' column. The result is a dataset of 14 variables that are weakly correlated and of ecological relevance.

Figure S3. Principal components of the Full dataset. A: Blue bars are eigenvalues, and the red line indicates the cumulative explained variance by all PCs up to this number (secondary *y*-axis). A dashed line indicates the Kaiser rule threshold of $\lambda=1$ for relevant principal components. B–D: Loadings on the first three principal components. For overview, only the first 20 variables are displayed. Variables are colour-coded by category (legend in panel C). Absolute *y*-axis values are for comparison only and indicate the loading onto the principal component.

Figure S4. Examples of noise score assignment using our modified nearest neighbour noise detection for $K=4$. The point with a black cross in the centre is the one receiving the noise score, indicated under the circle. The circle represents the maximum distance to its neighbours: αR. The noise score is 0 (not mislabelled) and 1 (likely mislabelled). (1, top left) All neighbours have a different label. This point is, therefore, likely mislabelled. (2) Point has only K/2 neighbours; this limits the maximum noise score to 0.5, and since all neighbours have a different label, the maximum noise score of 0.5 is assigned. (3) Feature outlier that has no neighbours and this canot be considered mislabelled. (4–6) Closeness of a point to members of the other class modulates how likely it will be considered noise. The shade indicates a hypothetic class decision boundary.

Figure S5. Finding optimal noise detection hyperparameters for random forest using the F0.5 score that penalises false positives (excluding a valid point) stronger than false negatives (missing a noisy point). A: Values of F0.5 score over alpha and *K* values with the optimal value highlighted at $K^*=20$ and $\text{Alpha}^*=1.5$. B: Performance for $K^*=20$ over the cut-off of data. The optimal F0.5 score is at 11.3% cut-off at $\text{Alpha}^*=1.5$. C: Comparison of the influence of using L1 versus L2 distance norm during noise detection at K^* and Alpha^*. L1 shows slightly improved performance.

Table S2. Values of hyperparameters that were compared during hyperparameter tuning for each classifier.

Figure S6. Visualisation of the similarity surface method for *Geniostoma ligustrifolium*, a North Island shrub. A: Distance D of average climatic and topographic conditions to the occurrence set. Coral dots are plots where the species has been observed. Darker colours are areas of higher similarity or shorter distances. Possible outliers are marked to visualise the need for the 95% cut-off. (For contrast, distances above 25 have been set to 25) B: Distribution of distances with 95% percentile marked (S′). Since the distance is an average across all years and climatic variables fluctuate, the mean is not very close to zero. C: The final similarity mask with the 95% percentile (S′) in orange and the additional area gained by upscaling S to S′ in yellow. Grey areas are excluded from prediction.

Figure S7. Relation of Difficulty score to species and predictive variables. A. Average difficulty by species ordered by mean difficulty for the Random Forest classifier. Means of other classifiers shown as lines. Bars indicate the number of observations for this species (secondary *Y* axis). B. Pearson correlation of Random Forests's numeric difficulty with variables from the 'Reduced' set of variables. Each point in the box plot represents a species. dY variable is the number of years between measurements. C: Correlation of mean difficulty with class imbalance (ratio of 'Increase' points vs all points).

Figure S8. Analysis of the susceptibility of the regression to the mean (RTM) effect following (Mazalla & Diekmann, 2022). Each data point consists of an abundance measurement at two time points a_1, a_0. RTM strength is assessed by correlating the species average abundance $a_{\text{Avg}} = \frac{1}{2}(a_1 + a_0)$ with the binary class label (i.e. increase or decrease in abundance, as implemented in this study in orange) or the continuous change score $\Delta_a = a_1 - a_0$ (i.e. abundance difference). (A) Histogram of the correlation R^2 for the binary and continuous case. (B) Bar plot of *p*-values for the same evaluation indicating whether a correlation, and thus the RTM effect, exists.

Figure S9. Analysis of the distributions of change in number of individuals across all observation pairs in the training data. (A) Change in abundance across all species standardised to zero mean and unit variance ($\tilde{p}(s)$, grey lines), average for all species (blue line) and a Gaussian fit to the average (red line). The average changes in abundance are close to Gaussian but with heavier tails. (B) Distribution of Kullback–Leibler divergences of species abundance changes $\tilde{p}(s)$ to a uniform distribution (blue line) and a Gaussian distribution (orange line). Changes in abundance $\tilde{p}(s)$ resemble a Gaussian distribution more closely than a uniform distribution.

Figure S10. Jaccard similarity between plot surveys by the time between surveys. High values indicate similar species composition. A: For a dataset of tagged woody plants. B: For the RECCE dataset that measures a much wider range of species (also non-woody) in height and cover tiers. Trendlines are rolling averages over a 15(A) and 10 (B) year window, respectively.

Table S3. Two measurements of the same plot in 2012 as part of different projects. Project 1 measured biodiversity, and Project 2 measured carbon. As a result, we suspect that shrubs were excluded.

Table S4. Results of the analysis of two measurements of the same plot where a species of a genus is 'replaced' by another species of the same genus. For example, in the last row, '*Veronica parviflora*' was detected in the first survey of a plot (first column). In 63.6% of the results, it was detected in the second survey of this plot (some years later). But in 9.1% of the cases, *V. leiophylla* was recorded while *V. parviflora* disappeared (second column). This indicates possible misclassification. The remaining 27.3% are cases where neither *V. parviflora* nor any other Veronica species was present in the second survey. Note that Coprosma 'small-leaved' was excluded from the final dataset and kept here as an illustration of the classification difficulty of the Coprosma genus.

Figure S11. Prediction accuracy of the dataset split by difficulty categories of the random forest classifier. Accuracy is the ratio of correctly classified instances to the total number of training instances.

Figure S12. Classifier performance on different sets of variables using the Abundance and DBH Dataset. A: Mean AUC scores over three variable sets. B and C: Cumulative canopy cover and number of species of all species classified with an AUC score above 0.7 over the fraction of noise removed. A single legend is used for all panels.

Table S5. Individual AUC scores for the random forest model on the Abundance Only dataset (at 10% label noise reduction) and Abundance and DBH dataset (at 15% reduction). The total cover of each species is given in the right-most column. Since data-deficient species are not included, the cover column sums up to ~73% of forest cover and the Abundance Only dataset contains fewer species. The table is sorted by Abundance and DBH score. (Scores below 0.7 are included due to rounding precision).

Figure S13. Learnability of the dataset. Each point in the box plots is a species. Acronyms describe the different models (Section S1.4). (A) Models trained on trivial, trivial + learnable or full (sub) datasets (see Section 2.8). (B) Fraction of trivial, learnable and unlearnable data points. (C) Similarity of difficulty labels between pairs of classifiers (left) and all (non-linear) classifiers (right).

Figure S14. Synthetic species generation for a hypothetical species shifting abundance towards higher elevation (A), latitude (B) or lower precipitation (C). The Gaussian sampling distributions for the years 2000 and 2019 (dashed lines) are determined using the mean and standard deviation of the distribution of all plots (black line). Their offset simulates a species abundance shift along the gradient of this variable. The distributions of the 1000 sampled plots are displayed as solid lines. They can be seen as the elevational, latitudinal or precipitation distribution in the years 1990 and 2019, with an abundance relocation towards higher values occurring during this time period.

Figure S15. ATI predictions for the synthetic species with an abundance gradient towards higher precipitation (A) or elevation (B) or latitude (C). As well as the average precipitation, elevation and latitude (D–F) in the study area and time period.

Figure S16. Correlation of predicted ATI values for the three synthetic species with the environmental predictor variables. The highest correlation values, as would be expected, occur with the variables used to generate the synthetic species themselves.

Table S6. Test statistics for statistical significance testing of abundance gradients in Figure 3. Values with $p < 0.05$ highlighted in bold.

How to cite this article: Shabanov, I., Lensen, A., Tonkin, J., & Deslippe, J. R. (2026). A machine learning framework for mapping shifts in species' abundance from long-term monitoring data. *Journal of Ecology*, *114*, e70344. https://doi.org/10.1111/1365-2745.70344